Eur. Phys. J. D **10**, 157–164 (2000)

THE EUROPEAN PHYSICAL JOURNAL D

EDP Sciences

Green function approximation and path integral numerical methods

A. Orlandi[1,a], M. Rosa-Clot[2], and S. Taddei[2]

[1] Dipartimento di Fisica, Università degli Studi di Modena e Reggio Emilia, and Istituto Nazionale di Fisica della Materia, Sezione di Modena, Via Campi 213a, 41100, Modena, Italy
[2] Dipartimento di Fisica, Università degli Studi di Firenze, and Istituto Nazionale di Fisica Nucleare, Sezione di Firenze, Largo Enrico Fermi 2, 50125, Firenze, Italy

Received 1st March 1999 and Received in final form 20 September 1999

Abstract. We evaluate the short time Green function by a series expansion of the exponent. The resulting expression allows the computation of the energy eigenvalues and eigenvectors of a quantum system with a very high precision. As an example, we show the comparison between the numerical results and the analytical solutions for harmonic and multi-well potentials both in one and two dimensions.

PACS. 02.70.-c Computational techniques – 31.15.Kb Path-integral methods

1 Introduction

A deterministic numerical method based on the path integral formalism [1] has been recently used to solve with remarkable precision low dimensional problems in quantum mechanics [2–6], and stochastic calculus [7]. The method allows to obtain the eigenvalues and the eigenfunctions of a quantum system, and the expectation values on random paths. It has good stability, good convergence properties, and a precision at least equivalent to that of efficient Hamiltonian methods (see, for instance, Ref. [4], for a comparison with a Fourier grid Hamiltonian method). In particular, it gives very high accuracy in delicate tunneling problems, where the localization properties of the wave functions are important as, for example, in the study of the electronic spectra of stacked semiconductor quantum dots [6]. The starting point of this technique is the short time Green function of the Schrödinger or the Fokker-Planck equation, in the case of quantum mechanics or stochastic calculus, respectively. An explicit exact expression for the short time Green function is not known in the general case, but we can write some approximate expressions. The accuracy of the numerical method clearly depends on such approximations. In this paper, we discuss a general technique to get an approximation for the propagator correct up to any given order in the time step, ε.

In Section 2, we briefly describe the deterministic numerical method in quantum mechanics, where the bound state energies, and wave functions are obtained by a direct diagonalization of the short time evolution operator. Since the short time propagator is dominated by a Gaussian, the corresponding matrix is sparse with the most significative elements centered around the diagonal, and can be efficiently diagonalized with algorithms for sparse matrices. In Section 3, we discuss the exponent expansion of the Green function. Finally, in Section 4 we give some examples, and compare the numerical results to the analytical solutions.

[a] e-mail: orlandi@saturno.unimo.it

2 Green function deterministic numerical method

The time evolution of the wave function is described by the propagator $K(x,t;y,t_0)$ according to the integral equation

$$\psi(\mathbf{x},t) = \int K(\mathbf{x},t;\mathbf{y},t_0)\psi(\mathbf{y},t_0)\mathrm{d}\mathbf{y}, \quad t \geq t_0. \tag{1}$$

Let us consider a one dimensional quantum system, described by a time independent Hamiltonian. The application of equation (1) to the stationary states of the system brings to

$$\int_{-\infty}^{+\infty} K(x,t;y,t_0)\psi_n(y)\mathrm{d}y = \mathrm{e}^{-\mathrm{i}E_n(t-t_0)/\hbar}\,\psi_n(x). \tag{2}$$

This is an integral eigenvalue problem, which can be transformed, by using a numerical integration formula, into

$$\sum_{j=1}^{N} w_j\, K_{ij}^{t,t_0}\, \psi_j^n \simeq \mathrm{e}^{-E_n(t-t_0)/\hbar}\,\psi_i^n, \tag{3}$$

where w_j are the weights associated to the integration rule and $K_{ij}^{t,t_0} = K(x_i,t;y_j,t_0)$.

In the passage from equation (2) to equation (3) we used the Euclidean formalism by substituting $(t-t_0) \mapsto -\mathrm{i}(t-t_0)$. Therefore we deal with Gaussian integrals which allow a more efficient numerical treatment.

Once the discretized propagator has been put in matrix form, the equation (3) can be solved by diagonalization, obtaining the energy levels and the corresponding wave functions, discretized in N points, from the eigenvalues and the eigenvectors, respectively.

The errors which affect this method are of two main kinds.

1. *Approximation of the propagator*
   The exact expression of $K(x,t;y,t_0)$ is known only in a few cases. For this reason, our target is to calculate, with various degrees of approximation, the so called short-time propagator, $K(x,t;y,t_0)$ when $(t-t_0)=\varepsilon$ is small. If the Hamiltonian is of the form
   $$\hat{H} = \hat{T} + \hat{V} = \frac{\hat{\mathbf{p}}^2}{2M} + V(\hat{\mathbf{x}}), \tag{4}$$
   then the short-time propagator, in the Euclidean formalism, can be written as
   $$K(\mathbf{x},t+\varepsilon;\mathbf{y},t) = \left(\frac{M}{2\hbar\pi\mathrm{i}\varepsilon}\right)^{d/2} \times \exp\left\{-\frac{1}{\hbar}\left[\frac{M(\mathbf{x}-\mathbf{y})^2}{2\varepsilon} + f(\mathbf{x},\mathbf{y};\varepsilon)\right]\right\}. \tag{5}$$
   The factor, $M(\mathbf{x}-\mathbf{y})^2/2\hbar\varepsilon$, represents the kinetic term, while in general the exact form of the potential term $f(\mathbf{x},\mathbf{y};\varepsilon)$ is unknown, and we must use an approximate expression. The most commonly used is the Feynman prescription,
   $$f(\mathbf{x},\mathbf{y};\varepsilon) \simeq \varepsilon\,\frac{V(\mathbf{x})+V(\mathbf{y})}{2}, \tag{6}$$
   which is good up to the second order in ε.
   In the next section will be described a computational technique to determine systematically higher order approximations of $f(\mathbf{x},\mathbf{y};\varepsilon)$.
2. *Numerical integration*
   The substitution of the integral between $\pm\infty$ with a finite sum introduces two types of errors.
   (a) A discretization error, depending on the integration rule. The Gaussian form of the propagator and the fact that the Gaussian centers move along the integration interval, compel us to use the trapezoidal rule, with constant weights $w_j = \delta x$ of the order of the Gaussian width, that is $\sqrt{\hbar\varepsilon/M}$. In practice, a ratio $\hbar\varepsilon/M\delta x^2 = 1$ gives an accuracy greater than 1%, and already with 1.25 we get at least 8 digits.
   (b) To work with matrices of finite dimensions is equivalent to put the system in an infinite potential well. The corrections to the energies and wave functions are negligible only for the states which are bounded inside the interval of discretization $[-L,L]$.

In the multi-dimensional case ($d>1$) the problem is the same, but the matrices to be diagonalized have dimension $N^d \times N^d$ and this is a severe limit to the method which can be practically used only for $d \leq 4$.

3 Exponent expansion for the short time propagator

Since for an accurate numerical integration we must take $\delta x \sim \sqrt{\hbar\varepsilon/M}$, once the space step δx has been fixed, ε cannot be taken arbitrarily small. Therefore it is important to use accurate approximations of the short time propagator. In Section 3.1 we give a brief review of the time powers expansion of reference [9], while in Section 3.2 we describe an extension of this approach.

3.1 Time powers expansion

Let $K(\mathbf{x},t+\varepsilon;\mathbf{y},t)$ be the Green function satisfying the Schrödinger equation

$$-\hbar\frac{\partial}{\partial\varepsilon}K(\mathbf{x},t+\varepsilon;\mathbf{y},t) = \left[-\frac{\hbar^2}{2M}\Delta_{\mathbf{x}} + V(\mathbf{x})\right] \times K(\mathbf{x},t+\varepsilon;\mathbf{y},t). \tag{7}$$

If we insert in (7) the expression (5), we get [8,9]

$$\frac{\partial f}{\partial\varepsilon} + \frac{(\mathbf{x}-\mathbf{y})}{\varepsilon}(\nabla_{\mathbf{x}} f) - \frac{\hbar}{2M}(\Delta_{\mathbf{x}} f) + \frac{1}{2M}(\nabla_{\mathbf{x}} f)^2 = V(\mathbf{x}). \tag{8}$$

If now we search for a solution in the form

$$f(\mathbf{x},\mathbf{y};\varepsilon) = \sum_{n=0}^{\infty} f_n(\mathbf{x},\mathbf{y})\varepsilon^n, \tag{9}$$

we obtain a recursive system of differential equations,

$$n f_n(\mathbf{x},\mathbf{y}) + (\mathbf{x}-\mathbf{y})\nabla_{\mathbf{x}} f_n(\mathbf{x},\mathbf{y}) = W_n(\mathbf{x},\mathbf{y}) \qquad n = 1,2,\ldots \tag{10}$$

where

$$W_n = \delta_{n1}V(\mathbf{x}) + \frac{\hbar}{2M}(\Delta_{\mathbf{x}} f_{n-1}) - \frac{1}{2M}\sum_{k=1}^{n-1}(\nabla_{\mathbf{x}} f_k)(\nabla_{\mathbf{x}} f_{n-k-1}). \tag{11}$$

The approximant f_0 is determined putting equal to zero the singular term in ε^{-1}. If the Hamiltonian contains a potential depending only on the coordinates (see Eq. (4)), we find

$$\nabla_{\mathbf{x}} f_0 = 0 \;\Rightarrow\; f_0 = \text{constant}. \tag{12}$$

The term, f_0, is an integration constant, and we can take $f_0 = 0$. After that f_0 has been fixed, the others can be obtained recursively by

$$f_n(\mathbf{x},\mathbf{y}) = \frac{1}{|\mathbf{x}-\mathbf{y}|^n}\int_\gamma |\mathbf{z}_\gamma - \mathbf{y}|^{n-1} W_n(\mathbf{z}_\gamma - \mathbf{y})\,\mathrm{d}\gamma = \int_0^1 \xi^{n-1} W_n(\mathbf{y} + \xi(\mathbf{x}-\mathbf{y}),\mathbf{y})\,\mathrm{d}\xi \qquad n = 1,2,\ldots, \tag{13}$$

where γ is the oriented segment from $\mathbf{y}$ to $\mathbf{x}$, and we have introduced $\mathbf{z}_\gamma = \mathbf{y} + \xi(\mathbf{x} - \mathbf{y})$, with $0 \leq \xi \leq 1$.

The explicit expressions of the first three approximants for the one-dimensional case are given by

$$f_1(x,y) = \frac{1}{x-y}\int_y^x V(z)\mathrm{d}z = \langle V\rangle(x,y) \tag{14}$$

$$f_2(x,y) = \frac{\hbar}{M(x-y)^2}\left[\frac{V(x)+V(y)}{2} - \langle V\rangle(x,y)\right] \tag{15}$$

$$f_3(x,y) = \frac{1}{2M(x-y)^2}\left[\langle V\rangle^2(x,y) - \langle V^2\rangle(x,y)\right] + \frac{\hbar^2}{M^2(x-y)^2}\left[-\frac{3M}{\hbar}f_2(x,y) + \frac{V'(x)-V'(y)}{4(x-y)}\right] \tag{16}$$

where $\langle V\rangle(x,y)$ and $\langle V^2\rangle(x,y)$ are the mean value in the interval between y and x of $V(z)$ and $V^2(z)$, respectively, and V' is the derivative of V.

The functions f_n depend on the initial and final points (y and x) and their diagonal values ($x = y$) are related to the Wigner approximants of the partition function of the system [10].

Vector potential

If a magnetic field is present the Hamiltonian is given by

$$\hat{H} = \frac{[\hat{\mathbf{p}} - \mathbf{A}(\hat{\mathbf{x}})]^2}{2M} + V(\hat{\mathbf{x}}), \tag{17}$$

where $\mathbf{A}(\hat{\mathbf{x}})$ is the vector potential. In this case equation (12) for the zero order term becomes

$$\nabla_{\mathbf{x}} f_0(\mathbf{x},\mathbf{y}) = -\frac{1}{M}\,\mathbf{A}(\mathbf{x}), \tag{18}$$

and the solution can be written as

$$f_0(\mathbf{x},\mathbf{y}) = -\frac{1}{M}(\mathbf{x}-\mathbf{y})\int_0^1 \xi\,\mathbf{A}(\mathbf{y}+\xi(\mathbf{x}-\mathbf{y}))\mathrm{d}\xi. \tag{19}$$

The approximants of higher order can be determined exactly in the same way by the equations (10, 11), that are not modified [8,9].

3.2 Space and time powers expansion

It has to be pointed out that the complexity of the exact calculation of the approximants increases with n and becomes quickly prohibitive. This is due to the non linear structure of the recursive system.

However the Euclidean short-time propagator is sensibly different from zero only if $|\mathbf{x}-\mathbf{y}|$ is of the order of $\sqrt{\hbar\varepsilon/M}$. This allows us to expand the $f_n(\mathbf{x},\mathbf{y})$ in powers of $(\mathbf{x}-\mathbf{y})$ [2] and to simplify the final result.

For the sake of simplicity, let us consider the one-dimensional case

$$f_n(x,y) = \frac{1}{(x-y)^n}\int_y^x (z-y)^{n-1} W_n(z,y)\mathrm{d}z \qquad n = 1,2,\ldots \tag{20}$$

We introduce $\Delta = (x-y)$ and we search a solution in the form

$$f_n(x,y) = \sum_{m=0}^{+\infty} f_{mn}(y)\;\Delta^m. \tag{21}$$

Accordingly with it we expand also the potential around the initial point y

$$V(y+\Delta) = \sum_{m=0}^{+\infty}\frac{V^{(m)}(y)}{m!}\;\Delta^m. \tag{22}$$

Since $W_1(x,y) = V(x)$ we obtain

$$f_{m1}(y) = \frac{V^{(m)}(y)}{(m+1)!}\,. \tag{23}$$

In a similar way, substituting (21) in (11) and the result in (20) we have

$$f_{mn}(y) = \frac{1}{2M}\hbar\frac{(m+2)(m+1)}{m+n}\;f_{m+2,n-1}(y) - \frac{1}{2M}\sum_{k=1}^{n-1}\sum_{i=1}^{m+1}\frac{i(m-i+2)}{m+n}f_{ik}(y)f_{m-i+2,n-k-1}(y). \tag{24}$$

In this way the approximation of $f(x,y;\varepsilon)$ up to the n_0th order is given in the form

$$f(\Delta,y;\varepsilon) = \sum_{n=0}^{n_0}\sum_{m=0}^{2(n_0-n)} f_{mn}(y)\;\Delta^m\;\varepsilon^n + O(\varepsilon^{n_0+1}) \tag{25}$$

where the truncation of the sum in m is made according with the fact that $(x-y)$ is of the order of $\sqrt{\hbar\varepsilon/M}$.

Two problems arise:

1. equation (25) is not symmetric in x and y (this introduces problems in numerical calculations);
2. the procedure shown above is not easily generalizable to the multi-dimensional case.

We can overcame both these difficulties by expanding the potential around the midpoint $\bar{x} = (x+y)/2$. We get

$$W_1(z,y) = V(z) = \sum_{m=0}^{+\infty}\frac{V^{(m)}(\bar{x})}{m!}\;(z-\bar{x})^m, \tag{26}$$

and by using (20)

$$f_1(x,y) = \sum_{k=0}^{+\infty}\frac{V^{(2k)}(\bar{x})}{(2k+1)!}\;\left(\frac{x-y}{2}\right)^{2k}. \tag{27}$$

Let us suppose we have computed all the first $n-1$ approximants $f_h(x,y)$ in the form

$$f_h(x,y) = \sum_{m=0}^{+\infty} F_m^h(\bar{x})\ (x-y)^m \quad h = 0, 1, \ldots, n-1. \tag{28}$$

To determine $W_n(z,y)$ we apply (11), differentiating also the coefficients $F_m^h(\bar{x})$ which now depend on x. We get $W_n(z,y)$ in the form

$$W_n(z,y) = \sum_{m=0}^{+\infty} C_m^n(\bar{x}')\ (z-y)^m \tag{29}$$

where $\bar{x}' = (z+y)/2$.

To compute $f_n(x,y)$ by application of (20) we remind that also the coefficients $C_m^n(\bar{x}')$ depend on the variable of integration z. Then we expand $W_n(z,y)$ in powers of $\Delta\bar{x} = \bar{x}' - \bar{x} = (z+y)/2 - (x+y)/2 = (z-x)/2$, and substitute the expansion,

$$W_n(z,y) = \sum_{m=0}^{+\infty}\sum_{k=0}^{+\infty} C_{mk}^n(\bar{x})\ (\Delta\bar{x})^k\ (z-y)^m, \tag{30}$$

in (20). Therefore, we obtain

$$f_n(x,y) = \sum_{m=0}^{+\infty}\sum_{k=0}^{+\infty} C_{mk}^n(\bar{x})\ \left(\frac{-1}{2}\right)^k \times \frac{(n+m-1)!\ k!}{(n+m+k)!}\ (x-y)^{m+k}. \tag{31}$$

In practical applications the sums are truncated to a finite number of terms as in equation (25), but now after the truncation the expressions (27, 31) are symmetric in x, y, and even in the variable $(x-y)$.

The procedure of computation is recursive and can be implemented in a computer program. Note that if the potential is a polynomial its expansion in Δ contains only a finite number of terms.

Finally, we point out that the expansion in powers of Δ, and ε of the short-time propagator gives, after integration, an asymptotic series in ε. This means that the expansion cannot be made indefinitely. In fact, when ε is too large and the points x, y are far apart, the high order terms in Δ are not suppressed by the Gaussian factor $\mathrm{e}^{-M\Delta^2/2\hbar\varepsilon}$. Thus Δ cannot be considered of order $\sqrt{\hbar\varepsilon/M}$ any more. Consequently large peaks appear on the borders of the short-time propagator matrix giving incorrect results. In other words the series above are not convergent. However, we can attain very high precision for ε small enough.

Multi-dimensional case

This procedure can be generalized also to the multi-dimensional case and the results can be written in synthetic way using multi-indices

$$\mathbf{k} = (k_1, k_2, \ldots, k_d)$$
$$\mathbf{k}! = k_1!\ k_2! \ldots k_d!$$
$$|\mathbf{k}| = k_1 + k_2 + \ldots + k_d,$$

where d is the dimension of the problem. We have for the first term

$$f_1(\mathbf{x},\mathbf{y}) = \sum_{\mathbf{k}=0}^{+\infty(e)} \frac{V^{(\mathbf{k})}(\bar{\mathbf{x}})}{\mathbf{k}!}\frac{2^{-|\mathbf{k}|}}{|\mathbf{k}|+1}\left[\prod_{i=1}^{d}(x_i-y_i)^{k_i}\right], \tag{32}$$

where the apex (e) means that only the terms with $|\mathbf{k}|$ even are summed and $\mathbf{x}$ and $\mathbf{y}$ are d-component vectors. The nth term is given by

$$f_n(\mathbf{x},\mathbf{y}) = \sum_{\mathbf{k},\mathbf{h}=0}^{+\infty} C_{\mathbf{kh}}^n(\bar{\mathbf{x}})(-2)^{-|\mathbf{h}|}\frac{[(n+|\mathbf{k}|-1)!](|\mathbf{h}|!)}{(n+|\mathbf{k}|+|\mathbf{h}|)!} \times \left[\prod_{i=1}^{d}(x_i-y_i)^{k_i+h_i}\right], \tag{33}$$

where the coefficients $C_{\mathbf{kh}}^n(\bar{\mathbf{x}})$ are defined by the multiple expansion

$$W_n(\mathbf{z},\mathbf{y}) = \sum_{\mathbf{k},\mathbf{h}=0}^{+\infty} C_{\mathbf{k},\mathbf{h}}^n(\bar{\mathbf{x}})\left[\prod_{i=1}^{d}(z_i-y_i)^{k_i}(d\bar{x}_i)^{h_i}\right]. \tag{34}$$

The expansion described above can be also used to reduce the dimension of the matrices to be diagonalized, because it allows to obtain better accuracy with the same number of grid points, but also the same accuracy with a lower number of points. This fact can be useful in the multi-dimensional case, where the matrix dimensions reach quickly critical values.

4 Applications

4.1 Harmonic oscillator

The harmonic oscillator, defined by

$$\hat{H} = \frac{\hat{\mathbf{P}}^2}{2M} + \frac{M\omega^2}{2}\hat{\mathbf{x}}^2, \tag{35}$$

has analytical solutions for the propagator, for the energy levels, and for the eigenfunctions. This allows us to test the numerical efficiency of the above expansion.

Let us consider the one dimensional case, and take $M=1$, $\omega=1$, and $\hbar=1$. The exact propagator is

$$K(x,t;y,t_0) = \sqrt{\frac{1}{2\pi\sinh\varepsilon}}\exp\left[\frac{(x^2+y^2)\cosh\varepsilon - 2xy}{2\sinh\varepsilon}\right] = \frac{1}{\sqrt{2\pi\varepsilon}}\exp\left\{-\frac{\Delta^2}{2\varepsilon} - \left[A(\varepsilon)\bar{x}^2 + B(\varepsilon)\Delta^2 + C(\varepsilon)\right]\right\}, \tag{36}$$

where, $\varepsilon = t - t_0$, $\Delta = x - y$, $\bar{x} = (x+y)/2$, and we have introduced the functions

$$A(\varepsilon) = \frac{1}{\tanh\varepsilon} - \frac{1}{\sinh\varepsilon} \tag{37}$$

$$B(\varepsilon) = -\frac{1}{2\varepsilon} + \frac{1}{4}\left(\frac{1}{\tanh\varepsilon} + \frac{1}{\sinh\varepsilon}\right) \tag{38}$$

$$C(\varepsilon) = \frac{1}{2}\ln\left(\frac{\sinh\varepsilon}{\varepsilon}\right). \tag{39}$$

By expanding in power series of ε,

$$K(x,t';y,t) = \frac{1}{\sqrt{2\pi\varepsilon}} \times \exp\left\{-\frac{\Delta^2}{2\varepsilon} - \left[\sum_{n=0}^{+\infty}\left(A_n\bar{x}^2 + B_n\Delta^2 + C_n\right)\varepsilon^n\right]\right\}, \tag{40}$$

we find

$$\begin{cases} f_n(x,y) = A_n\bar{x}^2 + B_n\Delta^2 & n \text{ odd} \\ f_n(x,y) = C_n & n \text{ even.} \end{cases} \tag{41}$$

As an example we write below the first ten approximants:

$$f_1(x,y) = \left(\frac{\Delta^2}{24} + \frac{\bar{x}^2}{2}\right) \quad f_2(x,y) = \frac{1}{12}$$

$$f_3(x,y) = \left(\frac{-\Delta^2}{1440} - \frac{\bar{x}^2}{24}\right) \quad f_4(x,y) = \frac{-1}{360}$$

$$f_5(x,y) = \left(\frac{\Delta^2}{60480} + \frac{\bar{x}^2}{240}\right) \quad f_6(x,y) = \frac{1}{5670}$$

$$f_7(x,y) = \left(\frac{-\Delta^2}{2419200} - \frac{17\bar{x}^2}{40320}\right) \quad f_8(x,y) = \frac{-1}{75600}$$

$$f_9(x,y) = \left(\frac{\Delta^2}{95800320} + \frac{31\bar{x}^2}{725760}\right) \quad f_{10}(x,y) = \frac{1}{935550}. \tag{42}$$

These expressions should be compared with the series expansion of the functions $A(\varepsilon)$, $B(\varepsilon)$, and $C(\varepsilon)$

$$A(\varepsilon) = \frac{\varepsilon}{2} - \frac{\varepsilon^3}{24} + \frac{\varepsilon^5}{240} - \frac{17\,\varepsilon^7}{40320} + \frac{31\,\varepsilon^9}{725760} + O(\varepsilon^{11})$$

$$B(\varepsilon) = \frac{\varepsilon}{24} - \frac{\varepsilon^3}{1440} + \frac{\varepsilon^5}{60480} - \frac{\varepsilon^7}{2419200} + \frac{\varepsilon^9}{95800320} - O(\varepsilon^{11})$$

$$C(\varepsilon) = \frac{\varepsilon^2}{12} - \frac{\varepsilon^4}{360} + \frac{\varepsilon^6}{5670} - \frac{\varepsilon^8}{75600} + \frac{\varepsilon^{10}}{935550} - O(\varepsilon^{11}). \tag{43}$$

Let us consider the eigenvalues obtained diagonalizing the propagator computed with several approximants.

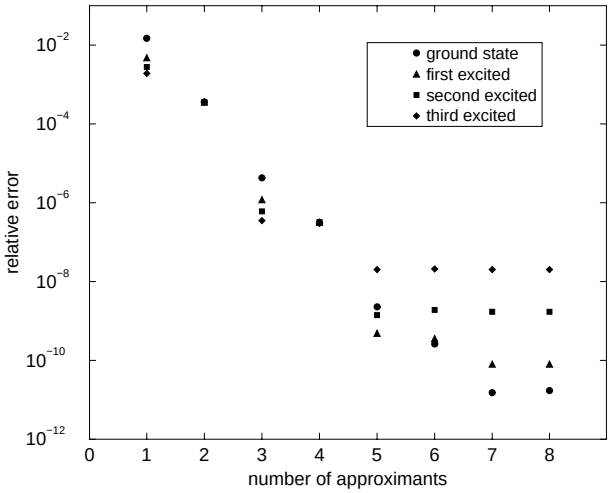

Fig. 1. The relative errors *versus* the number of approximants for the first four energy levels of the one-dimensional harmonic oscillator. The number of points is 41, and the discretization interval is $[-5, 5]$.

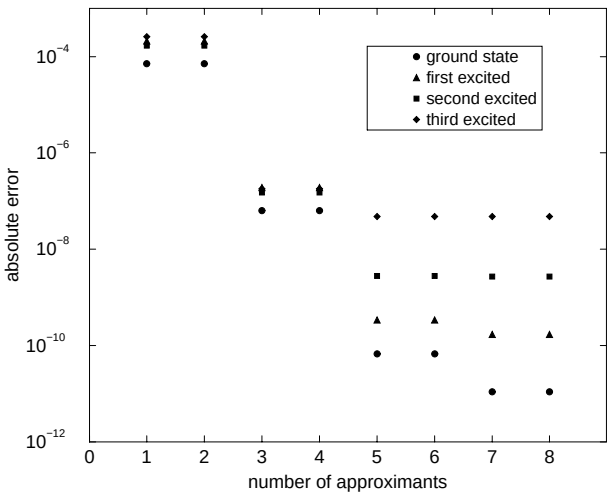

Fig. 2. The maximum absolute error *versus* the number of approximants for the first four stationary state wave functions of the one-dimensional harmonic oscillator. The number of points is 41, and the discretization interval is $[-4, 4]$.

In Figure 1, it is plotted the relative error $|\Delta E_n|/E_n$ for the first four energy levels *versus* the number of approximants.

Initially we gain about one order of magnitude for each added approximant, then there is a stabilization of the error around the value obtained by diagonalizing the exact propagator (36). The precision obtained for the first levels is very high (about $10 \div 11$ digits), notwithstanding the relatively small number of discretization points. Higher eigenvalues have more delocalized wave functions and are affected by errors due to the finite size of the discretization interval.

The description of the wave functions is very good. In Figure 2 it is shown the maximum absolute error, $\max_{j=1,\ldots,N} \left| |\psi_j^n|^2 - |\psi_n(x_j)|^2 \right|$, *versus* the number of

Table 1. Two-dimensional harmonic oscillator: energy levels, and corresponding relative errors. No. of points = 24 × 24, discretization interval = $[-5,5] \times [-5,5]$, $\varepsilon \simeq 0.28$, no. of approximants = 10.

Levels	Energy	Relative error
0	0.99999999992	8×10^{-11}
1	1.99999999957	2×10^{-10}
	1.99999999958	2×10^{-10}
2	2.99999999803	7×10^{-10}
	2.99999999803	7×10^{-10}
	2.99999999922	3×10^{-10}
3	3.99999999746	6×10^{-10}
	3.99999999748	6×10^{-10}
	3.99999999765	6×10^{-10}
	3.99999999766	6×10^{-10}
4	4.99999999642	7×10^{-10}
	4.99999999700	6×10^{-10}
	4.99999999702	6×10^{-10}
	5.00000006611	1×10^{-8}
	5.00000006627	1×10^{-8}

approximants, where ψ_j^n, and $\psi_n(x_j)$ are the numerical and the analytical eigenfunctions, respectively.

The results obtained with the approximants converge to those obtained with the exact propagator.

If a higher precision is needed, we must increase the number of discretization points N and/or enlarge the discretization interval $[-L, L]$. The increase in N (decrease of δx and of $\varepsilon \sim \delta x^2$) causes an enhancement of the convergence and the precision for all levels, so we get smaller errors with fewer approximants. The enlargement of the interval improves the results for higher levels, that have more delocalized wave functions.

In two dimensions we get results as good as those in one dimension. For example, in Table 1 are reported the first energy levels computed with ten approximants. It can be noticed that the degeneracy of the two dimensional harmonic oscillator is well described. In the multi-dimensional case the dimensionality of the matrices to be diagonalized become quickly critical. However, as far as it is possible to test the method, the results are similar.

4.2 One-dimensional double well

A particle of mass M, moves in the symmetric double well potential

$$V(x) = -Zx^2 + \lambda x^4, \quad Z, \lambda > 0. \tag{44}$$

The expressions of the first four approximants to the potential term of the Green function's exponent are (with $\hbar = 1$ and generic mass M)

$$f_1(x,y) = (-2Z)\left(\frac{\Delta^2}{24} + \frac{\bar{x}^2}{2}\right) + \lambda\left(\frac{\Delta^4}{80} + \frac{\Delta^2\,\bar{x}^2}{2} + \bar{x}^4\right)$$

$$f_2(x,y) = (-2Z)\left(\frac{1}{12\,M}\right) + \lambda\left(\frac{\Delta^2}{20\,M} + \frac{\bar{x}^2}{M}\right)$$

$$f_3(x,y) = (-2Z)^2\left(-\frac{\Delta^2}{1440\,M} - \frac{\bar{x}^2}{24\,M}\right) + \lambda\left(\frac{1}{10\,M^2} + \frac{\Delta^4\,Z}{1680\,M} + \frac{\Delta^2\,\bar{x}^2\,Z}{15\,M} + \frac{\bar{x}^4\,Z}{3\,M}\right) + \lambda^2\left(\frac{-\Delta^6}{7200\,M} - \frac{\Delta^4\,\bar{x}^2}{40\,M} - \frac{3\,\Delta^2\,\bar{x}^4}{10\,M} - \frac{2\,\bar{x}^6}{3\,M}\right)$$

$$f_4(x,y) = (-2Z)^2\left(-\frac{1}{360\,M^2}\right) + \lambda\left(\frac{\Delta^2\,Z}{210\,M^2} + \frac{4\,\bar{x}^2\,Z}{15\,M^2}\right) + \lambda^2\left(\frac{-\Delta^4}{600\,M^2} - \frac{\Delta^2\,\bar{x}^2}{5\,M^2} - \frac{6\,\bar{x}^4}{5\,M^2}\right).$$

We recognize the contributions due to the quadratic term and the terms in λ, that make the expression more and more complex as the order increase: this is due to the non linear form of the equations (10, 11) whose complexity increases with n.

Table 2. One-dimensional double well: values of the first four energy levels. The parameters are $Z = 5$, $\lambda = 0.5$ and $M = 0.5$. (a) No. of points = 41, discretization interval = $[-4, 4]$, no. of approximants = 12. (b) Reference [11].

Levels	Energy$^{(a)}$	Energy$^{(b)}$
0	−9.4469792	−9.44697938474047282
1	−9.4456297	−9.44562992836759352
2	−3.9215339	−3.92153584540274875
3	−3.8208697	−3.82087184715860094

In the case $Z = 5$, $\lambda = 0.5$, and $M = 0.5$ the first energy levels are known with high precision [11]. In Table 2, we make a comparison of them with our results.

In Figure 3 are plotted the relative errors $|\Delta E_n|/E_n$. As in the case of the oscillator we gain an order of magnitude for each added approximant and then the error tends to stabilize to the value affected only by the numerical integration. The precision is very high for all the first eleven levels and it allows to appreciate the very small splitting (due to the tunnel effect) between the first two couples of levels.

4.3 Two-dimensional multi-well potential

Let us consider the following two dimensional generalization of the potential

$$V(x) = -(Z_1\,x_1^2 + Z_2\,x_2^2) + \lambda\left(x_1^4 + 2a_{12}\,x_1^2x_2^2 + x_2^4\right), \quad Z_i, \lambda > 0. \tag{45}$$

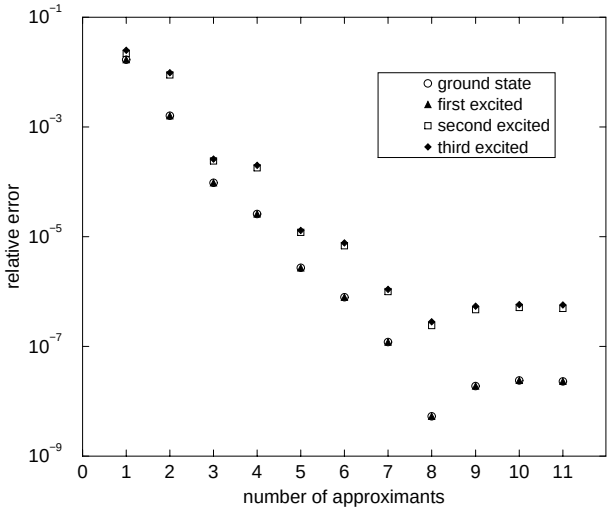

Fig. 3. The relative errors *versus* the number of approximants for the first four energy levels of the one-dimensional double well ($Z = 5$, $\lambda = 0.5$). The number of points is 41, and the discretization interval is $[-4, 4]$.

If $a_{12} = 0$ the problem is separable in two one-dimensional motions, correspondingly the propagator is factorizable in two one-dimensional parts and the approximants can be written as a sum of the corresponding terms. This can be seen by comparing

$$f_1(\mathbf{x},\mathbf{y}) = -\frac{Z_1\,{\Delta_1}^2}{12} - \frac{Z_2\,{\Delta_2}^2}{12} - Z_1\,\bar{x}_1^2 - Z_2\,\bar{x}_2^2$$

$$+\lambda\left(\frac{{\Delta_1}^4}{80} + \frac{{\Delta_2}^4}{80} + \frac{{\Delta_1}^2\,\bar{x}_1^2}{2} + \frac{{\Delta_2}^2\,\bar{x}_2^2}{2} + \bar{x}_1^4 + \bar{x}_2^4\right)$$

with the corresponding results in one dimension.

If $a_{12} \neq 0$ the motions on the two axes are coupled and the the expression of the first approximant becomes

$$f_1(\mathbf{x},\mathbf{y}) = -\frac{Z_1\,{\Delta_1}^2}{12} - \frac{Z_2\,{\Delta_2}^2}{12} - Z_1\,\bar{x}_1^2 - Z_2\,\bar{x}_2^2$$
$$+\lambda\left[\frac{{\Delta_1}^4}{80} + \frac{{\Delta_2}^4}{80} + \frac{{\Delta_1}^2\,\bar{x}_1^2}{2} + \frac{{\Delta_2}^2\,\bar{x}_2^2}{2} + \bar{x}_1^4 + \bar{x}_2^4\right.$$
$$\left.+a_{12}\left(\frac{\Delta_1^2\,\Delta_2^2}{80} + \frac{\Delta_2^2\,\bar{x}_1^2}{12} + \frac{\Delta_1\,\Delta_2\,\bar{x}_1\,\bar{x}_2}{3} + \frac{\Delta_1^2\,\bar{x}_2^2}{12} + \bar{x}_1^2\,\bar{x}_2^2\right)\right].$$

In the cases $M = 0.5$, $Z_1 = 1.5$, $Z_2 = 2.5$, $\lambda = 5$, and $a_{12} = 0, 1$ (see Figs. 4a and 4b) the first energy levels are known with high precision [11]. In Table 3, we make a comparison of them with our results.

In Figures 5a and 5b the relative errors for the first four levels *versus* the number of approximants are plotted. The precision achieved is very high, except for the fourth level (in the case $a_{12} = 1$) where the numerical integration error can be reduced only enlarging the discretization interval, and increasing the number of discretization points.

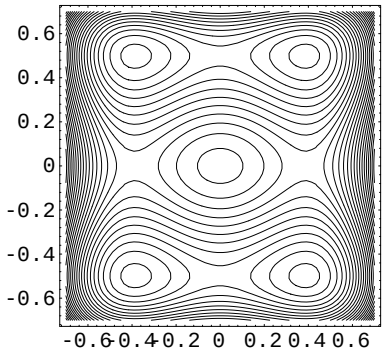

(a)

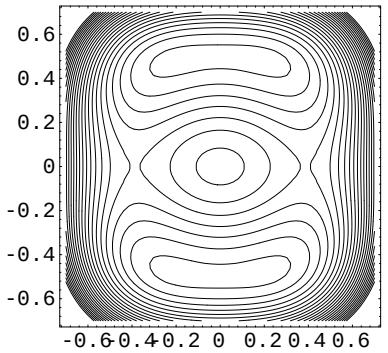

(b)

Fig. 4. Contour plots of the two-dimensional multi-well potential ($Z_1 = 1.5$, $Z_2 = 2.5$, $\lambda = 5$): (a) $a_{12} = 0$, (b) $a_{12} = 1$.

Tunneling in two dimensions

The sensitivity of the method in describing the various features of the tunnel effect in two dimensions emerges also when we look at the wave functions.

Let us consider the two-dimensional double well defined by the potential (45), with $a_{12} = 1$. In the case $Z_1 = 0.5$, $Z_2 = 4.0$, $\lambda = 0.5$ and $M = 0.5$ we have two identical wells, with minima aligned along the x_2 axis, at a distance given by

$$l = \sqrt{\frac{2Z_2}{\lambda}} = 4.0, \tag{46}$$

symmetrically posed with respect to the origin of the axes (see, Fig. 4b).

We can introduce a symmetry breaking applying a small perturbation that makes the two wells slightly different. For example we can consider a potential linearly dependent on x_2,

$$V(x) = -(Z_1\,x_1^2 + Z_2\,x_2^2) + \lambda\left(x_1^4 + 2a_{12}\,x_1^2x_2^2 + x_2^4\right)$$
$$+\left(\frac{\varphi}{l}\right)\,x_2, \quad Z_i, \lambda > 0. \tag{47}$$

We have evident effects on the wave functions also with very little values of φ, as we can see in Figure 6, where

Table 3. Two-dimensional multi-well potential: values of the first four energy levels. The parameters are $Z_1 = 1.5$, $Z_2 = 2.5$, $\lambda = 5$ and $M = 0.5$. (a) No. of points = 45×45, discretization interval = $[-2.5, 2.5] \times [-2.5, 2.5]$, no. of approximants = 4. (b) Reference [11].

	$a_{12} = 0$		$a_{12} = 1$	
Levels	Energy[(a)]	Energy[(b)]	Energy[(a)]	Energy[(b)]
0, 0	2.713132	2.71313903038	3.200734	3.20074097557
0, 1	6.579732	6.57975757558	7.670437	7.67047026747
1, 0	6.913580	6.91360663984	8.027127	8.02716125152
1, 1	10.78018	10.7802251850	13.35450	13.4183263417

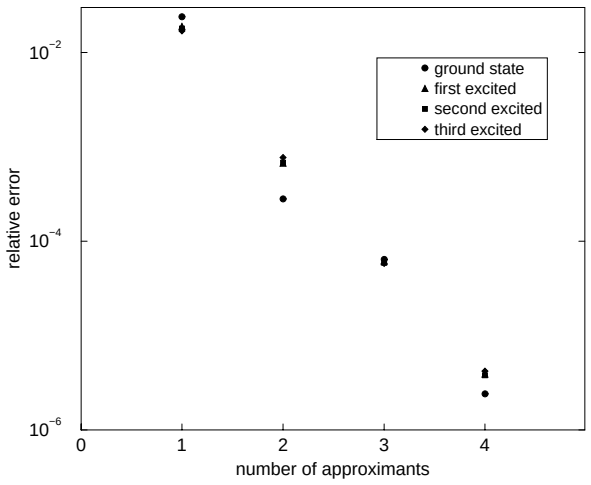

(a)

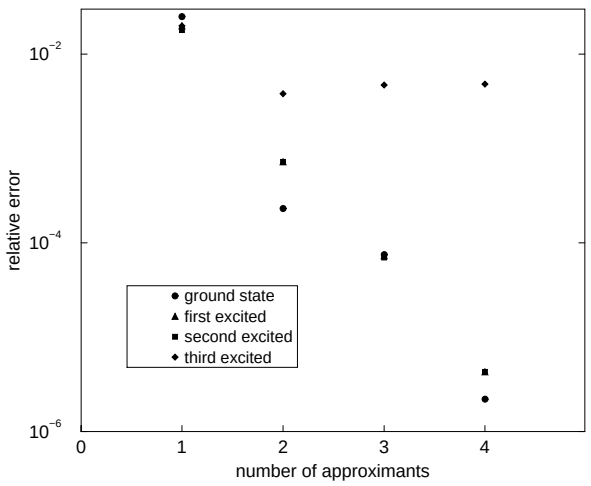

(b)

Fig. 5. The relative errors *versus* the number of approximants for the first four energy levels of the two-dimensional multi-well potential ($Z_1 = 1.5$, $Z_2 = 2.5$, $\lambda = 5$ and $M = 0.5$): (a) $a_{12} = 0$, (b) $a_{12} = 1$. The number of points is 45, and the discretization interval is $[-2.5, 2.5] \times [-2.5, 2.5]$.

we plot the numerical ground state wave function of the two-dimensional double well perturbed with a term of the order of 10^{-3}.

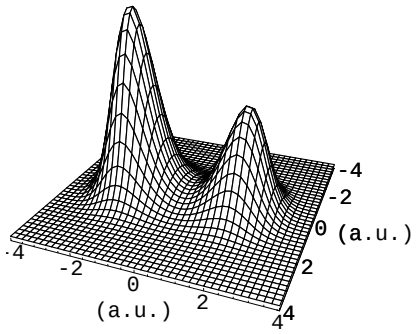

Fig. 6. Ground state wave function of the two-dimensional double well ($Z_1 = 0.5$, $Z_2 = 4.0$, $\lambda = 2.0$ and $M = 0.5$) with a symmetry breaking term ($\sim 10^{-3}$).

The asymmetry of the wave functions is not easily attained with other methods, when the perturbation is so little.

5 Conclusions

We have discussed the Green Function Deterministic Numerical Method and its reliability in giving eigenvalues and eigenvectors of one and two-dimensional quantum problems.

The critical point is the correctness of the Green Function for the finite time and space steps. For this reason we have developed a general method, which works in arbitrary dimension and gives the Green Function thorough an exponent expansion in Δx, and ε up to any arbitrary order.

This method is convergent, stable and limited only by the available computer memory.

Tests of the method have been performed for some specific potentials.

References

1. R.P. Feynman, A.R. Hibbs, *Quantum Mechanics and Path Integrals* (McGraw-Hill, New York, 1965).
2. M. Rosa-Clot, S. Taddei, Phys. Lett. A **197**, 1 (1995).
3. V.R. Manfredi *et al.*, Int. J. Mod. Phys. E **5**, 519 (1996).
4. S. Taddei, J. Comp. Phys. **134**, 62 (1997).
5. M. Colocci *et al.*, Appl. Phys. Lett. **70**, 3140 (1997).
6. M. Colocci *et al.*, Appl. Phys. Lett. **74**, 564 (1999).
7. M. Rosa-Clot, S. Taddei, `cond-mat/9901279`.
8. N. Makri, W.H. Miller, Chem. Phys. Lett. **151**, 1 (1988).
9. N. Makri, W.H. Miller, J. Chem. Phys. **90**, 904 (1989).
10. E. Wigner, Phys. Rev. **40**, 749 (1932).
11. M.R.M. Witwit, J. Comp. Phys. **123**, 369 (1996).